Effect of β-Ring Rotation on the Structures and Vibrational Spectra of β-Carotene: Density Functional Theory Analysis

Wei-Long Liu,[†] Zhi-Gang Wang,[‡,§] Zhi-Ren Zheng,*[,†] Ai-Hua Li,[†] and Wen-Hui Su[†,#]

Center for Condensed Matter Science and Technology, Department of Physics, Harbin Institute of Technology, Harbin 150001, China, Institute of Atomic and Molecular Physics, Ji Lin University, Changchun 130012, China, Shanghai Institute of Applied Physics, Chinese Academy of Sciences, P.O. Box 800-204, Shanghai 201800, China, and College of Physics, Ji Lin University, Changchun 130023, China

Received: March 7, 2008; Revised Manuscript Received: June 28, 2008

The effect of β-ring rotation on the structures and vibrational spectroscopic characteristics of β-carotene, including infrared (IR) intensities and Raman activities, is analyzed using density functional theory. Two stable isomers having *Ci* symmetry are obtained. The reversion of bond lengths is ascribed to the hyperconjugation effect. The natural bond orbital (NBO) charge analysis suggests that the NBO charges of C5 can be used to estimate the degree of π-electron delocalization. These structural variations are used to analyze and assign the vibrational spectra. It is concluded that (a) the similar rotational angle dependencies of ν1 and ν2 frequencies justify the contribution of C═C stretch vibrations to the ν2 mode and explain the same conjugation length dependencies of ν1 and ν2 frequencies in polyenes, (b) the ν1 mode can be assigned to the C═C stretching in the central part of polyene chain, whereas β-rings play an important role in ν2 and IR1 bands, especially for the all-trans isomer, and (c) the transition dipole moment of the calculated IR1 absorption band is relevant to the conjugation degree and the crossing angle between the eigenvectors of the polyene chain and the C5═C6 stretching vibration. This theoretical analysis, together with our previous Raman spectral experiments, suggests that the C6−C7 bond is easier to be twisted than other parts of β-carotene molecule and so provides an insight into the structures of carotenoids and the properties of binding sites in carotenoproteins.

Introduction

Density functional theory (DFT) has become very popular because of its good accuracy and reasonable computational cost. In comparison with ab initio calculations, the DFT method includes electron correlation via functions and is more biased toward π-electron delocalization.[1,2] Therefore, DFT can perform quite satisfactorily on conjugated molecules of moderate size, such as polyenes and carotinoids.

The trans−cis isomerization process for *all-trans*-undecaene, which was considered as a model of β-carotene, was investigated by DFT more than a decade ago.[3] A DFT study of the reaction mechanisms between singlet-oxygen and a carotenoid model was reported.[4] A set of carotenoid radical cations[5,6] and stereoisomers of spheroidene[7] were also calculated using DFT. DFT was recently applied to analyze the intramolecular charge-transfer state in protein complexes[8] and radical cations at the reaction center.[9,10]

The use of DFT to describe the vibrations of carotenoids molecules has been well established. Dokter et al. performed the DFT calculations on the model molecules of a series of isotope labeled *all-trans*-spheroidene and gave exact and minute assignments on the resonance Raman spectra.[11] Schlücker et al. reported the first DFT analysis on the structures and vibrational spectra of β-carotene.[12] The comparison between observed and calculated resonance Raman spectra suggested that besides the 15,15′-cis configuration there is another cis-configuration of spheroidene at the reaction center.[13] These results reveal the potential of DFT to explore the complicated systems.

Raman spectra are useful for characterization of carotenoid molecular configuration, binding state in proteins, and stereoisomers in particular.[13,14] The assignment of Raman modes is very important for better utilization of this information. Various methods such as normal-coordinate analysis[15] and isotope labeling are used for this purpose,[11,16] Although most Raman bands have been assigned, the explanations of some experimental observations are still under dispute. For example, the experimental Raman spectra show that both ν1 and ν2 bands of carotenoids shift to a lower frequency for a longer conjugated chain,[17] and this can not be explained using the conventional concept of π-electron delocalization if ν1 and ν2 bands are assigned to C═C and C−C stretching, respectively. Thus, Rimai et al. assigned ν2 band to the admixture of C−C and C═C stretching with C−H bending modes,[17] while Weesie et al. assigned this band to the superposition of C−H bend with significant intensity and C−C stretch with less intensity.[18]

Carotenoids with the same conjugated length always present similar Raman spectra. The conjugated chain is thus identified as the main contributor to the Raman spectra of all the carotenoids.[11,19] However, DFT analysis shows that the stabilities of a set of retinal derivatives are relevant to the type of substitution of the end groups.[2] It has also been demonstrated that the ring torsion effect is responsible for the higher stability of *s-cis*-β-carotene in comparison with its all-trans isomer.[12] The effect of headgroup rotation on the spin delocalization of the β-carotene radical cation[5] and on the stabilities and excitation

* To whom correspondence should be addressed. E-mail: zrzheng@hit.edu.cn. Phone: +86-451-8641-8440. Fax: +86-451-8641-8440.
† Harbin Institute of Technology.
‡ Institute of Atomic and Molecular Physics, Ji Lin University.
§ Chinese Academy of Sciences.
# College of Physics, Ji Lin University.

10.1021/jp802024v CCC: $40.75
Published on Web 09/27/2008

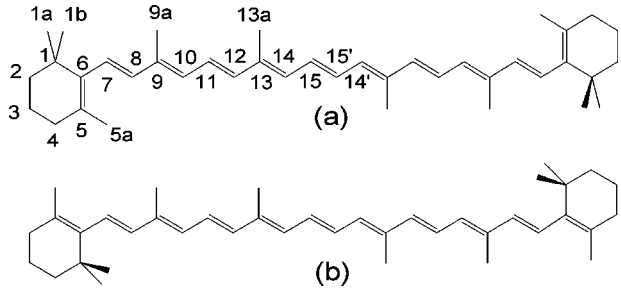

Figure 1. Constitution formulas of (a) *s-cis* and (b) *all-trans-β*-carotene.

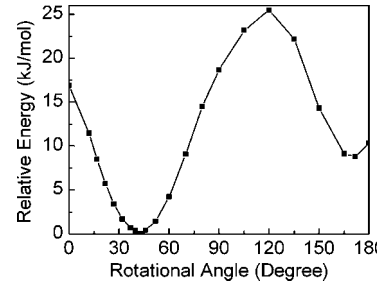

Figure 2. Potential energy curve for rotation around C6−C7 and C6′−C7′ bonds.

energies of xanthophylls[20] have also been reported. These results indicate that the end groups, especially the β-rings of β-carotene analogues, inevitably have their influence on the stability and vibrational spectrum of carotenoids. Therefore, the effect of β-ring rotation on neutral β-carotene is investigated using DFT to explore the relationship between the structures and vibrational properties of carotenoids in depth. These analyses can provide a novel insight into the interpretation of carotenoid vibrational spectra.

Computational Details

Although most calculations were performed using the hybrid DFT method, such as B3LYP, the first DFT and vibrational spectroscopic analysis of β-carotene was performed using pure density functional BPW91.[12] Therefore, all the calculations reported in the present study were carried out using BPW91 and the 6−31G(d) basis set, as implemented in the Gaussian 03 program package.[21]

The rotation of the β-rings was performed by freezing the ∠C5−C6−C7−C8 (∠C5′−C6′−C7′−C8′) dihedral angle at an angle from 0° to 180° (−180°) and optimizing all the other degrees of freedom. Symmetry constraints were used to keep the symmetry[12] of all the structures during optimization. The purpose of this work is not to reproduce the experimental spectra to a high precision but to reflect the general features and trends. So the frequencies[22] and intensities[12] of the vibrational spectra were not corrected.

Results and Discussion

A. Effect of Headgroup Rotation on Molecular Structures. ***(i) Optimized Molecular Structures.*** Two stable structures of β-carotene shown in Figure 1 are obtained without restricting the ∠C5−C6−C7−C8 dihedral angles. Although the structure shown in Figure 1a is usually referred to as 'all-trans', we call it 's-cis' structure to distinguish it from the structure shown in Figure 1b. The ∠C5−C6−C7−C8 dihedral angles are 42.9° and 171.6° for the two stable structures, respectively. The s-cis isomer is 8.8 kJ/mol more stable than the all-trans form. The optimized *s-cis-β*-carotene structure is in good agreement with the XRD data.[23] The small discrepancy between the observed and optimized dihedral angles of the periphery part of the conjugated chain can be attributed to the crystal packing forces.[18] The optimized s-cis and all-trans structures are almost the same as that reported by Schlücker et al.[12] (see the Supporting Information-I for details). This similarity justifies the reliability of our optimized structures and warrants the further calculations. All the optimized structures with frozen ∠C5−C6−C7−C8 dihedral angles adopt *Ci* symmetry. (The number of imaginary frequencies for these structures is presented in the Supporting Information-II.)

(ii) Potential Energy Curve. As shown in Figure 2, the potential energy varies sinusoidally with the rotational angle. The two minimums in the potential energy curve at 42.9° and 171.6° correspond to the s-cis and all-trans structures, respectively. The relative stabilities of the two structures have been demonstrated by Schlücker et al.[12] The energy barrier located at 120° for the transformation from all-trans to s-cis form is not every large (16.7 kJ/mol). This may also be the reason for the natural abundant β-carotene to adopt s-cis conformation. It is worth noting that if the headgroups are individually rather than simultaneously rotated, i.e. the structures are not constrained to keep the *Ci* symmetry, other minima in the potential energy surface are as shown by Druew.[20] This is beyond the scope of the present work and needs further analysis.

(iii) Bond Length and π-Electron Delocalization. It can be seen from Figure 3a and 3b that the bonds, which are most affected by the rotation are the ones closest to the headgroups. The double (single) bonds of the conjugated chain become gradually shorter (longer) as the dihedral angle increases from 0° to 90°. According to the common concept of π-electron delocalization, the bond lengths of double (single) bonds in the central part of the conjugated chain are longer (shorter) than those in the periphery. However, both experimental[23] and theoretical[12,18] results show that the presence of methyl groups in carotenoids perturbs this regulation; the methylated double and single bonds are longer than the nonmethylated bonds. As shown in Figure 3, the bond length of C9═C10 (or C13═C14) is longer than C11═C12 (or C15═C15′), while C10−C11 is shorter than C12−C13. This reversion of bond length can be explained by the hyperconjugation effect, which originates from the powerful pull by the methyl on the π-electrons of the conjugated chain. It is this effect that elongates the methylated C═C and C−C bonds. It can be seen from Figure 3 that the differences between bond lengths C9═C10 and C11═C12, C13═C14 and C15═C15′, and C10−C11 and C12−C13 for the 90° structures are a little smaller than those for the 0° and 180° structures, which suggests that the hyperconjugation effect is stronger and the conjugation degree is weaker when the β-rings are perpendicular to the conjugated chain. The effect of headgroup rotation on the bond length of C9−C9a shown in Figure 3b also indicates a stronger hyperconjugation effect for the perpendicular structure.

The degree of π-electron delocalization (conjugation) in a molecule can be evaluated by means of the bond length alternation (BLA) parameter, which is defined as the total length difference between single bonds and double bonds.[1,6] The BLA parameter decreases as the conjugation degree increases. In order to evaluate the effect of headgroup rotation on the degree of π-electron delocalization, BLA_{5-15} for all the isomers has been calculated and presented in Figure 3c. It can be seen from Figure 3c that the BLA values for the perpendicular structures (around 90°) are much larger than those for the planar ones (around 0°

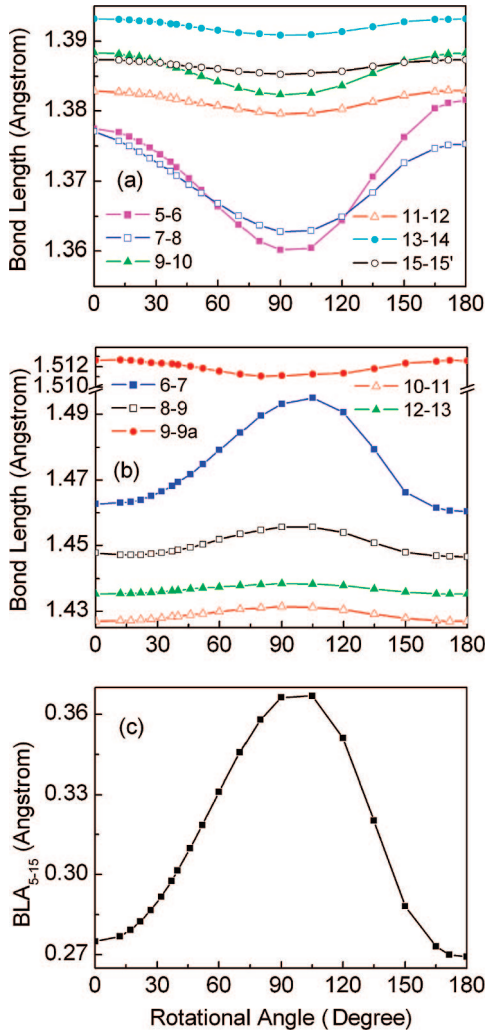

Figure 3. Dependence of (a) C═C and (b) C−C bond lengths and (c) BLA_{5-15} on rotational angle.

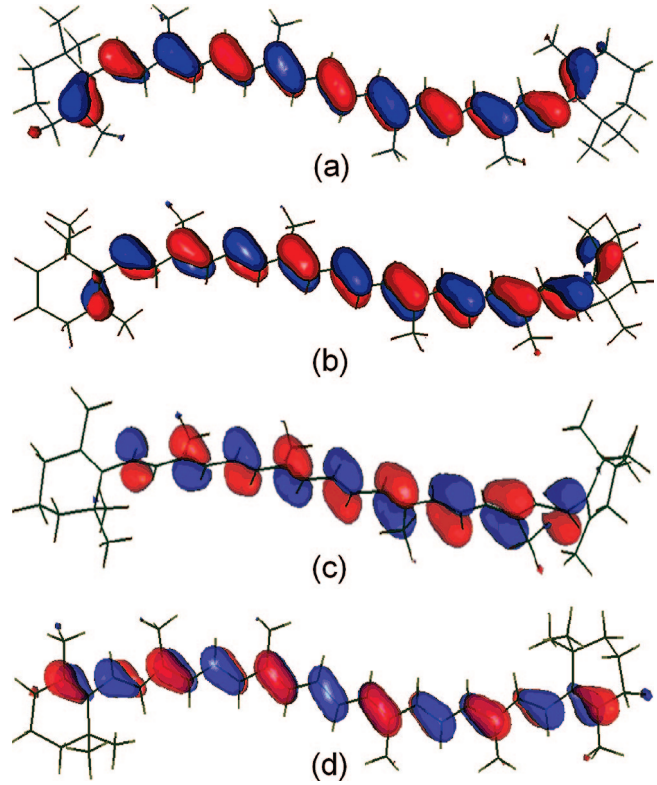

Figure 4. Schematic representation of the highest occupied molecular orbital of representative structures: (a) 0°, (b) s-cis, (c) 90°, and (d) 180°.

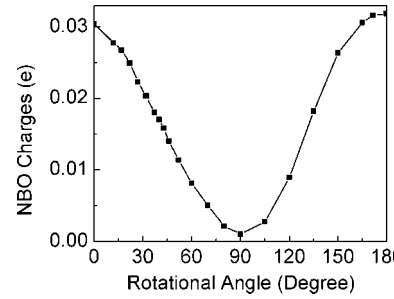

Figure 5. Dependence of NBO charges of C5 on the rotational angle.

and 180°), and so the π-electron delocalization is gradually broken as the ∠C5−C6−C7−C8 dihedral angle is twisted from 0° to 90°. In addition, the slightly larger BLA for the 0° isomer compared with that for the 180° form indicates that the conjugation degree of the former is lower than that of the latter. It can be clearly seen from Figure 4 that, for the planar isomers, the degree of electron delocalization is much larger than that of the perpendicular form, which is in good agreement with the BLA calculations.

In order to clearly show the variation of π-electron delocalization, we analyzed the NBO charges of the carbon atom (C5) located at the end of the conjugated chain. It can be seen from Figure 5 that the electrons move toward C5 to show the weakening of π-electron delocalization as the end ring rotates from 0° to 90°, which implies that the NBO charges of the terminal carbon atom of the conjugated chain (C5 for β-carotene) can be used to estimate the degree of π-electron delocalization. Since NBO charges of C5 are positive, more C5 charges mean a stronger delocalization. This criterion is better than BLA because it provides a direct means for evaluating the delocalization degree in the conjugated chain of carotenoids with different lengths.

B. Effect of Molecular Structure on Vibrational Spectra. ***(i) Raman Spectra.*** The experimental Raman spectrum of crystalline β-carotene is dominated by three bands located around 1520, 1160, and 1005 cm^{-1} and are called ν1, ν2, and ν3 bands, respectively. A weak band, which appears around 960 cm^{-1} in solution and is called the ν4 band.[24] The frequency and intensity of the ν1 mode shown in Figure 6 are directly obtained from the DFT calculations. For the ν2 mode, two bands of appreciable intensity are obtained in the 1176−1190 cm^{-1} region when the rotational angle is larger than 135° and the intensity-weighted average frequency[11] and the total intensity are taken as shown in Figure 6.

The frequency of the ν1 mode undergoes an obvious increase as the β-ring is rotated from 0° to 90°. The similar angle dependences of ν1 frequency and BLA reveal the intrinsic association between the ν1 mode and π-electron delocalization. The frequency of the ν1 mode depends on the conjugation degree, and the ν1 frequency decreases as the conjugation increases. It is not difficult to explain this relationship from the viewpoint of π-electron delocalization if ν1 mode is assigned to the C═C stretch vibrations.[17,18] It should be noted that the BLA value of 180° isomer is a little smaller than that of the 0° isomer, while the ν1 frequency of the former is a little higher than that of the latter because the difference of BLAs originates mainly from the peripheral parts of the conjugated chain, and

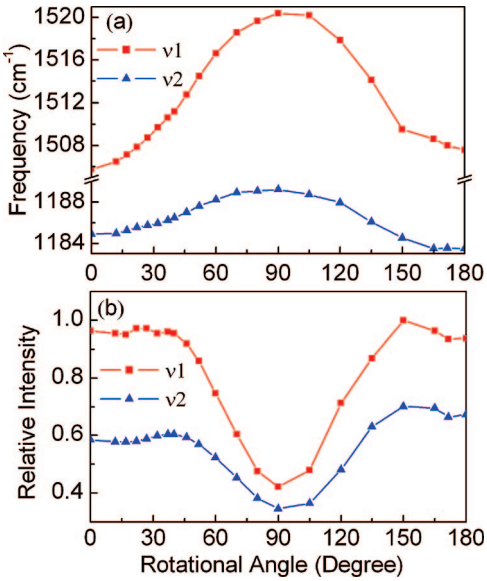

Figure 6. Dependence of (a) frequency and (b) relative intensity of ν1 and ν2 modes on the rotational angle.

the contribution of the peripheral C═C stretch vibrations to the ν1 mode is rather small. This is in good agreement with normal-coordinate analysis, which assigned the ν1 mode to the C═C stretch vibrations in the central part of the conjugated chain.[15]

If the ν2 mode is assigned to the C−C stretch vibrations, the frequencies of ν1 and ν2 modes should shift toward the opposite direction according to the theory of π-electron delocalization. However, both experimental[17] and calculated [25]results show that the ν1 and ν2 modes shift simultaneously to lower (higher) frequencies as the conjugation chain get longer (shorter). Rimai et al. demonstrated that all the Raman-active modes are sufficiently admixed with C═C stretching to ensure their resonance enhancement, and the ν2 mode cannot be distinguished by a unique contribution of C−C bonds.[17] It can therefore be concluded that the ν2 mode is a mixture of C−C and C═C stretching coupled with C−H in-plane bending. Although the C−C stretching plays a principal role in determining the ν2 frequency,[15] the frequency variations induced by the headgroup rotation are dominated by the C═C bonds. Accordingly, the frequency variation is smaller for ν2 mode than that for ν1 mode.

Figure 6b shows that the intensities of ν1 and ν2 modes present similar angle dependences. The obvious decreases in the intensities of both modes for the perpendicular configurations can be ascribed to the reduced conjugation degree, which decreases the changes in polarizability corresponding to the C−C and C═C stretches. The intensities of both modes fluctuate to a small extent before 40° and after 135°. This is attributed to the small changes in the molecular structure and π-electron delocalization in these angle ranges. The rotational angle dependence of the ν1 intensity is quite symmetrical. However, the ν2 intensity of the 180° isomer is visibly enhanced compared with that of the 0° form. This discrepancy justifies the contribution of C−C stretches in the β-rings to the ν2 mode for the isomers whose ∠C5−C6−C7−C8 dihedral angle is larger than 135°.

We did not find any regular angle dependence of ν3 and ν4 frequencies from the DFT calculations, while the intensity of ν4 mode shows an interesting curve with two maxima, as shown in Figure 7. The ν4 mode is assigned to the C−H out-of-plane (op) wagging in the peripheral parts of polyene chain.[15] It has

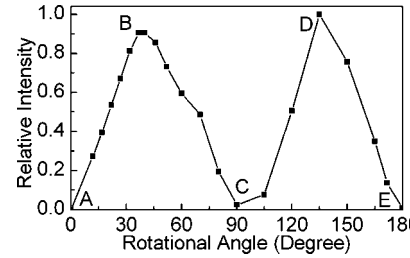

Figure 7. Dependence of relative intensity of the ν4 mode on the rotational angle.

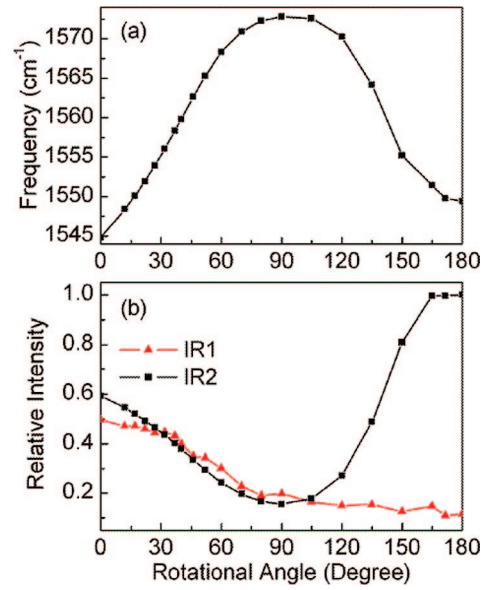

Figure 8. Dependence of (a) frequency of the IR1 mode and (b) relative intensity of IR1 and IR2 modes on the rotational angle.

been demonstrated that the intensity of this op vibration is associated with the distortion of the molecular conformation from the plane.[15] We can therefore deduce the configuration changes induced by the headgroup rotation. The obvious increase of the ν4 intensity before 40° (from A to B) indicates that the conjugation between β-rings and polyene chain is moderately strong; thus, the peripheral parts of polyene chain can rotate along with the rotation of β-rings. As the dihedral angle increases (from B to C) and the conjugation degree decreases, the peripheral parts of polyene chain gradually come back to the plane. As the angle is rotated from 90° to 180° (from C to E), the molecular structure undergoes a process inverse to that from A to C.

(ii) Infrared Spectra. Three representative modes located at 1559, 3053, and 977 cm^{-1} for the s-cis form are used to analyze the effect of molecular structure on the calculated infrared spectra and are called IR1, IR2, and IR3 modes, respectively. Two bands of appreciable intensity are obtained around 1560 cm^{-1} in the calculated IR spectra, and the intensity-weighted average frequency and the total intensity are taken for the IR1 mode. The rotational angle dependences of IR1 and IR2 modes are shown in Figure 8.

The IR1 mode is assigned to the C═C stretching of the conjugated chain.[14] Although the pattern of Figure 8a is similar to the angle dependence of the ν1 frequency, the variation of the IR1 mode is much larger than that of the ν1 mode. This means that the contribution of the peripheral double bonds to the IR1 band is much larger than that to the ν1 mode. It has been demonstrated that the intensity of the IR1 mode is determined by the crossing angle between the eigenvectors of

the polyene chain and the C5═C6 stretching vibration.[12] The crossing angle (α) between the C5═C6 and C═C double bonds in the polyene chain can be given by

$$\alpha = \cos^{-1}\left(\frac{3}{4}\cos\theta - \frac{1}{4}\right) \quad (1)$$

where θ is the ∠C5−C6−C7−C8 dihedral angle. When $\theta = 70.5°$, $|\cos\alpha| = 0$, the transition dipole moment of IR1 absorption should be its minimum. However, as shown in Figure 8b, the DFT calculated minimum locates at $\theta = 90°$. This means that the contribution of C5═C6 to the IR1 mode is very small when the π-electron delocalization between β-rings and polyene chain is broken, and then the absorption intensity is dependent on the conjugation degree of polyene chain. According to eq 1, the intensity of the IR1 absorption band for the 0° isomer is half of that for the 180° isomer, which is in agreement with the DFT calculated results shown in Figure 8b. Compared with the discrepancy for the 90° isomer, this consistency justifies the validity of eq 1 and suggests that the transition dipole moment of IR1 absorption is also dependent on the relative orientation between C5═C6 and the C═C stretching in polyene chain when the π-electron delocalization in the whole molecule is not broken.

As shown in Figure 8b, the intensity of IR2 mode is a monotonous decrease function of the rotational angle. The IR2 mode is assigned to the C−H stretch vibrations in the C1a and C1b methyl groups[12] and is independent of the conjugation degree. The eigenvectors of the polyene chain and the methyl H atoms are nearly parallel for the 0° isomer; in contrast, they are almost perpendicular for the 180° form.[12] Therefore, the resulting transition dipole moment of the IR2 mode for the 0° isomer is larger than that for the 180° form.

The strongest band observed in the experimental IR spectrum located at 977 cm^{-1} is assigned predominantly to the C−H op mode of the central part of polyene chain.[15] The calculated frequencies and intensities of this mode fluctuate in a very small range (data not shown) and accordingly confirm the conclusion that the headgroup rotation has its effect mainly on the peripheral parts of polyene chain.

Conclusions

We have in the present study characterized the effect of β-ring rotation on the structures and vibrational spectra of β-carotene through DFT analysis and obtained two stable structures of β-carotene. The small energy barrier for the transformation from all-trans to s-cis may be one of the reasons for the natural abundant β-carotene to adopt s-cis conformation. The structure, potential energy, and charge distribution of β-carotene molecule vary systematically as the ∠C5−C6−C7−C8 dihedral angle rotates from 0° to 180°. The configurational distortions of β-carotene result in the systematic variations of vibrational spectra. The detailed analyses of several representative Raman and IR bands can provide a novel insight into the assignment of carotenoid vibrational spectra.

Some clues are provided through the vibrational spectroscopic analysis in this work for the investigation of the structure of carotenoids or the properties of the binding sites in carotenoproteins. Our previous Raman spectral experiments show that, compared with those in solid state, both ν1 and ν2 bands shift to higher frequencies in solution, and the frequency shift of the ν1 mode is larger than that of the ν2 mode.[24] This provides evidence for the notion that the β-rings are slightly twisted when the molecular conformation is relaxed in solution and suggests that the C6−C7 bond is more easily rotated than the other parts of β-carotene molecule. Therefore, we speculate that the distortion around the C6−C7 bond of the β-carotene molecule in protein is more probable to occur. It has been established that the β-ring end of β-carotene is the main contributor to the interaction strength in the CH−π interactions, which are partly responsible for binding β-carotene in the photosynthetic pigment−protein complexes.[26] This CH−π interaction can bring about the torsion of β-rings and influence the vibrational spectra. For example, compared with that in solution, the increased ν1 frequency of β-carotene in photosystem II suggests that the β-rings are rotated in this system.[27] However, the ν1 frequencies of another β-carotene analogue, astaxanthin, shift to lower wavenumbers in proteins.[28] This result indicates that, besides the structural factors, the effect of the binding sites, such as charged groups and hydrogen bonds, should also be taken into account.[28]

It can therefore be concluded that our DFT analysis offers an illustrative means of investigating the molecular structures and vibrational characteristics of carotenoids, especially β-carotene analogues, in solutions and carotenoproteins.

Acknowledgment. Our special thanks go to Professor W. Kiefer and Doctor S. Schlücker for providing the optimized structure and vibrational spectrum of *s-cis-β*-carotene for reference. This work was supported by the National Natural Science Foundation of China (Grant Nos. 10774034 and 10674034), China Postdoctoral Science Foundation (Grant No. 20070420685), and Shanghai Postdoctoral Scientific Program (Grant No. 07R214159).

Supporting Information Available: I: Comparison among the reported experimental structures (ref 23), theoretical structures (ref 12), and our calculated structures by using DFT. II: Number of imaginary frequencies for all structures. III: Coordinates and energies of all the isomers discussed in this paper. IV: Rotational angle dependence of several representative vibrational modes (frequence and intensity). This information is available free of charge via the Internet at http://pubs.acs.org.

References and Notes

(1) Kertesz, M.; Choi, C. H.; Yang, S. J. *Chem. Rev.* **2005**, *105*, 3448.
(2) Terstrgen, F.; Buss, V. *J. Mol. Struct. (THEOCHEM.)* **1998**, *430*, 209.
(3) Bernardi, F.; Garavelli, M.; Olivucci, M.; Robb, M. A. *Mol. Phys.* **1997**, *92*, 359.
(4) Garavelli, M.; Bernardi, F.; Olivucci, M.; Robb, M. A. *J. Am. Chem. Soc.* **1998**, *120*, 10210.
(5) Himo, F. *J. Phys. Chem. A* **2001**, *105*, 7933.
(6) Guo, J. D.; Luo, Y.; Himo, F. *Chem. Phys. Lett.* **2002**, *366*, 73.
(7) Pendon, Z. D.; Sullivan1, J. O.; van der Hoef, I.; Lugtenburg, J.; Cua, A.; Bocian, D. F.; Birge, R. R.; Frank, H. A. *Photosynth. Res.* **2005**, *86*, 5.
(8) Vaswani, H. M.; Hsu, C. P.; Gordon, M. H.; Fleming, G. R. *J. Phys. Chem. B* **2003**, *107*, 7940.
(9) Gao, Y.; Focsan, A. L.; Kispert, L. D.; Dixon, D. A. *J. Phys. Chem. B* **2006**, *110*, 24750.
(10) Amarie, S.; Standfuss, J.; Barros, T.; Kühlbrandt, W.; Dreuw, A.; Wachtveitl, J. *J. Phys. Chem. B* **2007**, *111*, 3481.
(11) Dokter, A. M.; van Hemert, M. C.; Velt, C. M. I.; van der Hoef, K.; Lugtenburg, J.; Frank, H. A.; Groenen, E. J. J. *J. Phys. Chem. A* **2002**, *106*, 9463.
(12) Schlücker, S.; Szeghalmi, A.; Schmitt, M.; Popp, J.; Kiefer, W. *J. Raman Spectrosc.* **2003**, *34*, 413.
(13) Wirtz, A. C.; van Hemert, M. C.; Lugtenburg, J.; Frank, H. A.; Groenen, E. J. J. *Biophys. J.* **2007**, *93*, 981.
(14) Koyama, Y.; Kito, M.; Takii, T.; Saiki, K.; Tsukida, K.; Yamashita, J. *Biochim. Biophys. Acta* **1982**, *680*, 109.
(15) Saito, S.; Tasumi, M. *J. Raman Spectrosc.* **1983**, *14*, 310.
(16) Kuroda, Y. M.; Fujii, R.; Ko-chi, N.; Sashima, T.; Koyama, Y.; Abe, M.; Gebhard, R.; van der Hoef, I.; Lugtenburg, J. *J. Phys. Chem. A* **2002**, *106*, 3566.

(17) Rimai, L.; Heyde, M. E.; Gill, D. *J. Am. Chem. Soc.* **1973**, *95*, 4493.

(18) Weesie, R. J.; Merlin, J. C.; Lugtenburg, J.; Britton, G.; Jansen, F. J. H. M.; Cornard, J. P. *Biospectroscopy* **1999**, *5*, 19.

(19) Oliveira, L. F. C.; Dantas, S. O.; Velozo, E. S.; Santos, P. S.; Ribeiro, M. C. C. *J. Mol. Struct.* **1997**, *435*, 101.

(20) Dreuw, A. *J. Phys. Chem. A* **2006**, *110*, 4592.

(21) Frisch, M. J.; Trucks, G. W.; Schlegel, H. B.; Scuseria, G. E.; Robb, M. A.; Cheeseman, J. R.; Montgomery, J. A.; Vreven, T.; Kudin, K. N.; Burant, J. C.; Millam, J. M.; Iyengar, S. S.; Tomasi, J.; Barone, V.; Mennucci, B.; Cossi, M.; Scalmani, G.;Rega, N.; Petersson, G. A.; Nakatsuji, H.; Hada, M.; Ehara, M.; Toyota, K.; Fukuda, R.; Hasegawa, J.; Ishida, M.; Nakajima, T.; Honda, Y.; Kitao, O.; Nakai, H.; Klene, M.; Li, X.; Knox, J. E.; Hratchian, H. P.; Cross, J. B.; Bakken, V.; Adamo, C.; Jaramillo, J.; Gomperts, R.; Stratmann, R. E.; Yazyev, O.; Austin, A. J.; Cammi, R.; Pomelli, C.; Ochterski, J. W.; Ayala, P. Y.; Morokuma, K.; Voth, G. A.; Salvador, P.; Dannenberg, J. J.; Zakrzewski, V. G.; Dapprich, S.; Daniels, A. D.; Strain, M. C.; Farkas, O.; Malick, X.; Rabuck, A. D.; Raghavachari, K.; Foresman, J. B.; Ortiz, J. V.; Cui, Q.; Baboul, A. G.; Clifford, S.; Cioslowski, J.; Stefanov, B. B.; Liu, G.; Liashenko, A.; Piskorz, P.; Komaromi, I.; Martin, R. L.; Fox, D. J.; Keith, T.; Al-Laham, M. A.; Peng, C. Y.; Nanayakkara, A.; Challacombe, M.; Gill , P. M. W.; Johnson, B.; Chen, W.; Wong, M. W.; Gonzalez, C.; Pople, J. A. Gaussian 03, Revision D.01, Gaussian, Inc., Wallingford, CT, 2004.

(22) Merrick, J. P.; Moran, L. *J. Phys. Chem. A* **2007**, *111*, 11683.

(23) Senge, M. O.; Hope, H.; Smith, K. M. *Z. Naturforsch.* **1992**, *47c*, 474.

(24) Liu, W. L.; Zheng, Z. R.; Zhu, R. B.; Liu, Z. G.; Xu, D. P.; Yu, H. M.; Wu, W. Z.; Li, A. H.; Yang, Y. Q.; Su, W. H. *J. Phys. Chem. A* **2007**, *111*, 10044.

(25) Zerbetto, F.; Zgierski, M. Z. *Chem. Phys. Lett.* **1988**, *143*, 153.

(26) Wang, Y.; Mao, L.; Hu, X. *Biophys. J.* **2004**, *86*, 3097.

(27) Ghanotakis, D. F.; de Paula, J. C.; Demetriou, D. M.; Bowlby, N. R.; Petersen, J.; Babcock, G. T.; Yocum, C. F. *Biochim. Biophys. Acta* **1989**, *974*, 44.

(28) Merlin, J. C. *J. Raman Spectrosc.* **1987**, *18*, 519.

JP802024V